Digital signal processing in MIMO radars with time-multiplexed transmit signals

Borko B. Đaković[a], *Slobodan* M. Simić[b],
Lidija M. Trivundža[c], *Aleksandar* G. Ristić[d]

[a] Serbian Armed Forces, General Staff,
Telecommunications and Information Technology Directorate (J-6),
Center for Applied Mathematics and Electronics,
Belgrade, Republic of Serbia,
e-mail: borkodj2001@gmail.com, **corresponding author**,
ORCID iD: https://orcid.org/0009-0000-4662-3981

[b] University of Defence in Belgrade, Military Academy,
Department for Military Electronic Systems,
Belgrade, Republic of Serbia,
e-mail: slobodan.simic@va.mod.gov.rs,
ORCID iD: https://orcid.org/0000-0002-6846-4886

[c] Serbian Armed Forces, General Staff,
Development and Equipment Directorate (J-5),
Technical Test Center, Belgrade, Republic of Serbia,
e-mail: lidija.trivundza@gmail.com,
ORCID iD: https://orcid.org/0009-0004-7040-8586

[d] Ministry of Defence of the Republic of Serbia,
Military Technical Institute, Belgrade, Republic of Serbia,
e-mail: ristic1504@gmail.com,
ORCID iD: https://orcid.org/0009-0003-1994-2815

doi https://doi.org/10.5937/vojtehg73-54972

FIELD: digital signal processing, telecommunications, electronic, electromagnetic
ARTICLE TYPE: original scientific paper

Abstract:

Introduction/purpose: A current topic of significant research and development efforts in the field of radar systems is MIMO (Multiple-Input-Multiple-Output) radar technology. MIMO radars represent a revolutionary step forward in radar technology, as the use of multiple transmitting antennas that emit orthogonal waveforms enables improved detection and angular resolution. To achieve effective results, high-quality digital signal processing and the application of advanced algorithms are essential for obtaining target information. This paper places special emphasis on coherent MIMO radars, with the objective of enhancing angular resolution. Time-multiplexing of transmit signals is applied as a primary method to achieve orthogonality between signals, utilizing a Frequency Modulated Continuous Wave (FMCW) signal as the foundation for the transmit waveform. The aim of this paper is to provide and explain the fundamentals *of digital signal processing in MIMO radars, present analytical expressions, and validate them through simulation and experimental verification.*

Methods: The theoretical foundations are presented, with the Discrete Fourier Transform (DFT) used as a primary tool in digital signal processing to obtain information about the distance, velocity, and azimuth of the target. A simulation was developed in the MATLAB software package to analyze the performance of the radar system model. Experimental verification was conducted, where specific scenarios were recorded using the radar platform PUP_DUAL24P_T2R4, and the collected data was subsequently processed. The MATLAB functions MIMOFMCW and procDC were written to generate simulation samples of echo signals and to automate signal processing and the display of characteristic Range-Velocity and Range-Angle matrices.

Results: The simulation and experimental verification confirm the validity of the theoretical foundations related to digital signal processing in MIMO radars, and the target parameters can be clearly determined.

Conclusion: The Discrete Fourier Transform is a simple tool that provides satisfactory results for determining the range, velocity, and angle of targets. FMCW radars offer accuracy in determining range and velocity, while the MIMO mode enhances angular resolution. The DFT algorithm is capable of determining the target angle, but with a certain error, making the use of high-resolution methods necessary for more accurate angle determination.

Key words: MIMO, radar, TDM, FMCW, radar data cube, DFT, beat frequency, virtual antenna.

Introduction

MIMO radars are modern and advanced radar systems in which, unlike conventional radar systems, each transmitting antenna transmits an arbitrary waveform independently of other transmitting antennas. MIMO radars transmit uncorrelated signals in different directions or transmit mutually orthogonal signals in the same direction. Due to different waveforms and orthogonality between signals, receiving antennas can separate the echo signals originating from a target and assign them to a specific transmitter, which are then collected and further processed. This approach improves the probability of target detection and the accuracy of estimating the angle of arrival of echo signals (Stoica & Li, 2008; Wiesbeck et al, 2015).

MIMO technology has wide applications in telecommunications, significantly enhancing data transmission capacity and speed, particularly in 5G and 6G systems (Dessai & Patidar, 2024) through Massive MIMO technology (Wanga et al, 2021), which utilizes antenna arrays for spatial diversity (Abdi & Rasheed, 2022). This technology improves angular resolution and accuracy in radar systems (Janoudi et al, 2023), which is especially important for automotive radars in the mm-wave range, enabling clear detection of objects and supporting the development of unmanned vehicles and their communication with one another (Han et al, 2024). Additionally, MIMO technology is increasingly used in Synthetic Aperture Radar (SAR) systems for terrain imaging (Wu et al, 2019) and in medicine for monitoring human vital signs (Alizadeh et al, 2019), detection glucose levels (Omer et al, 2018) and detecting tumors (Bliss & Forsythe, 2006) using the mm-Wave radar.

One of the primary classifications of MIMO radars is based on the antenna configuration. Accordingly, they can be divided into MIMO radars with widely spaced antennas, or statistical MIMO radars, and MIMO radars with collocated antennas, or coherent MIMO radars (Sun, 2023).

In statistical MIMO radars, the transmit and receive antennas are widely separated, providing independent scattering responses for each antenna pair (Figure 1a). By positioning antennas at different locations, the target is illuminated from various angles, mitigating the effects of a reduced radar cross-section and a poor electromagnetic wave scattering response. This results in more robust detection performance and reduces the likelihood of missing the target. In the other case, the transmit and receive antennas of a coherent MIMO radar are positioned relatively close together (Figure 1b).

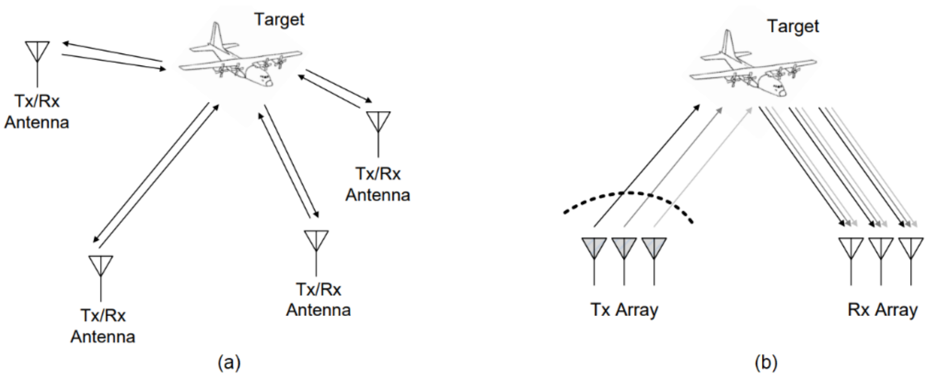

Figure 1 – Statistical MIMO radar (a) and coherent MIMO radar (b) (Sun,2023)

Here, it is assumed that the electromagnetic wave scattering response from the target is the same for each antenna pair, with minimal delay. The antennas of a MIMO radar transmit waveforms independently of each other. The goal is to use coherent signal processing to form a virtual array of antennas, providing improved estimation of the signal's angle of arrival. This approach ensures that fewer antennas can achieve the effect of a larger antenna array on reception, enhancing the radar's angular resolution (Stoica & Li, 2008; Sun, 2023; Davis et al, 2014).

To prevent signal interference during transmission and ensure that receivers can successfully distinguish and assign signals to the correct transmitter, it is necessary for the signals to be orthogonal to each other. Signal orthogonality significantly simplifies further processing. Typical methods of achieving orthogonality include using time-division multiplexing (TDM) (Sun et al, 2014), frequency-division multiplexing (FDM) (Liu, 2009), and code-division multiplexing (CDM) (He et al, 2009).

In time-division multiplexed signals (TDM), orthogonality is achieved by having the transmitting antennas emit signals at different times. While one antenna is transmitting, the other antennas do not emit any signal. This method is simple to implement as it can use a single transmitter and a microwave switch, but it requires precise time synchronization and, in this way, the full transmission capacity is not utilized (Sun et al, 2014).

Formation of virtual antennas in MIMO radars

MIMO coherent radars, by emitting mutually orthogonal waveforms, can form a virtual antenna array and thereby increase angular resolution without increasing the number of receiving antennas. Virtual antennas are formed by combining signals from multiple transmitters and receivers. The number of virtual antennas that can be achieved is:

$$N_{\mathrm{R}} = N_{\mathrm{T_x}} \cdot N_{\mathrm{R_x}} \tag{1}$$

where N_{Tx} is the number of transmitting antennas, and N_{Rx} is the number of receiving antennas. In MIMO radar systems with a linear antenna array, the transmitting antennas must be spaced at a distance of $d_{\mathrm{T_x}} = N_{\mathrm{R_x}} \cdot d_{\mathrm{R_x}}$, where N_{Rx} is the number of receiving antennas and d_{Rx} is the distance between receiving antennas.

By measuring the phase delays $\Delta\phi$ of the signals at the elements of the receiving antenna array, the angle at which the target is located is determined. In the case shown in Figure 2a), the second transmitting antenna, due to its distance from the reference transmitting antenna, introduces an additional phase shift of $4 \cdot \Delta\phi$. The signal from the first receiving antenna sent by the second transmitting antenna will be phase-shifted by $4 \cdot \Delta\phi$, which would correspond to the fifth receiving antenna. Using this approach, eight virtual receiving antennas are formed, whose signal model is equivalent to a physical scenario with one transmitter and eight receiver antennas (Figure 2b). This holds true assuming that the target is located in the far field relative to the antennas and that the reflected wave from the target reaches the receiving antennas as a plane wave (Rao, 2018).

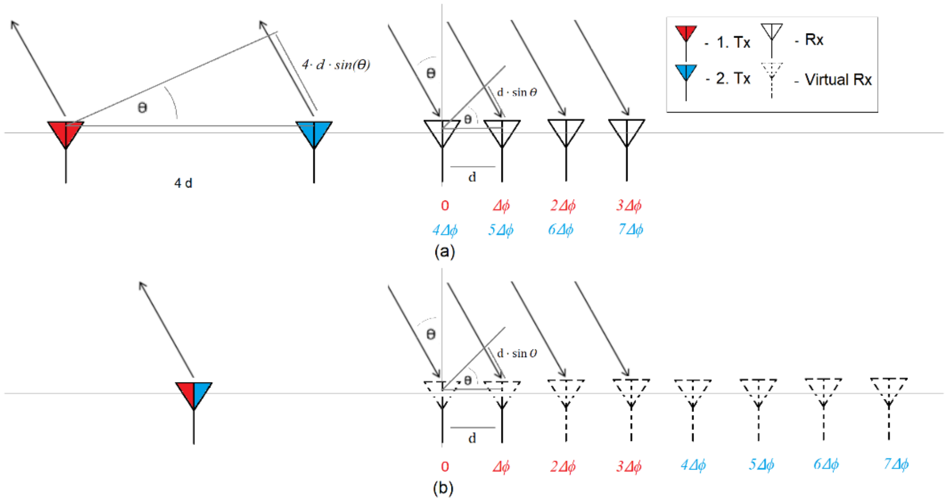

Figure 2 – MIMO Antenna Array (a) and Virtual Antenna Array(b)

Mathematical signal model in a coherent MIMO radar

The next chapter presents and explains the radar system model used in the research, as well as the form of the transmitted signal. The models were created based on the radar platform that was used at the end of the research for conducting experimental verification.

Model FMCW radar system

The signal generator generates the FMCW signal $x_T(t)$, which after the power amplifier (PA) is emitted from the transmitting antenna *T*x. After the signal hits the object, part of the signal energy is reflected from the object (echo signal) and returns back to the receiving antenna *R*x, where it is received as a signal $x_R(t)$ (Figure 3). After that, the signal $x_R(t)$ goes to the quadrature receiver, where it is mixed with the signal $x_T(t)$ and the signal $x_T(t)$ whose phase is shifted by 90º. In this way, two signals are obtained, one in phase (I Signal) and one in quadrature (Q Signal), which pass through a low-pass filter (LPF) after the mixer. In this way, an intermediate frequency (IF) signal is obtained, which after the analog-digital converter (ADC) is forwarded to digital signal processing (DSP), where the range, velocity, and azimuth of the target are determined (Mahafza, 2013).

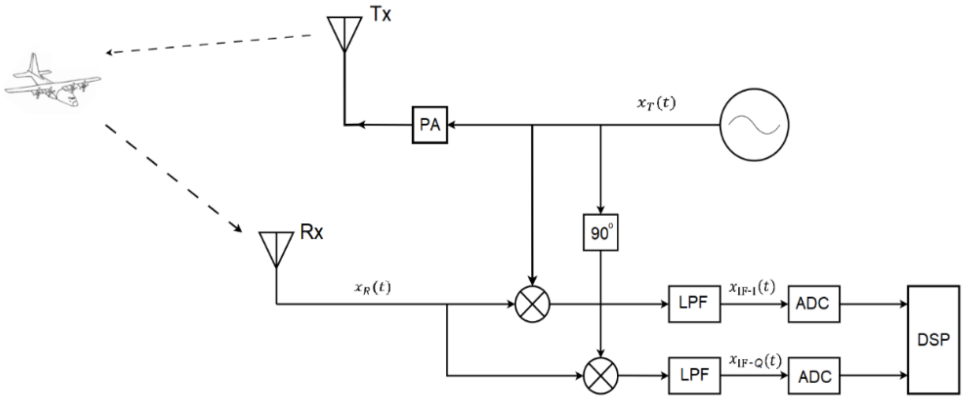

Figure 3 – Block diagram of the radar system

FMCW Signal

The radar system transmits a linearly increasing FMCW signal, which ensures a large product of signal duration and frequency bandwidth (*tB*), simultaneously enabling high range resolution and a high signal-to-noise ratio (Richards, 2014).

The characteristics of the FMCW signal are: the starting frequency f_c, the bandwidth *B,* the chirp signal duration T_C, and the ramp slope coefficient *S* (Figure 4). The ramp slope coefficient is calculated as (Iovescu & Rao, 2016):

$$S = \frac{B}{T_C}. \quad (2)$$

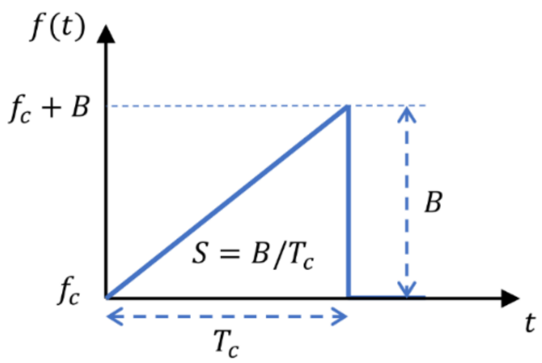

Figure 4 – FMCW chirp signal (Li et al, 2021)

The FMCW signal can be mathematically represented as (Li et al, 2021):

$$x_T = A_{\mathrm{T}} \cos(2\pi\, f_{\mathrm{C}}\, t \; + \; \pi\, S\, t^2), \tag{3}$$

while the instantaneous frequency is determined as (Li et al, 2021):

$$f(t) = \frac{1}{2\pi}\frac{d}{dt}(2\pi\, f_{\mathrm{c}}\, t \; + \; \pi\, S\, t^2) = f_{\mathrm{c}} + S\, t. \tag{4}$$

The radar system receives the echo signal $x_{\mathrm{R}}(t)$ in its receiver and mixes it with the transmit signal $x_{\mathrm{T}}(t)$ and $x_{\mathrm{T}}(t)$ phase-shifted by π/2. As the frequency of the transmitted FMCW signal $x_{\mathrm{T}}(t)$ increases linearly over time, at the moment when the echo signal $x_{\mathrm{T}}(t)$ arrives at the receiver, the frequencies $f_{\mathrm{T}}(t)$ and $f_{\mathrm{R}}(t)$ of the transmitted and received signals will not be the same (Figure 5a). The difference in frequencies occurs because the transmitted signal changes frequency during the time as the signal is emitted, reflected from the object, and returned to the receiver. After the mixer, the signals is fed to a low-pass filter. The low-pass filter passes the lower sideband of the signals, i.e., the signal component located at the frequency $f_{\mathrm{T}}(t)$-$f_{\mathrm{R}}(t)$, and removes the signal component located at the frequency $f_{\mathrm{T}}(t)$+$f_{\mathrm{R}}(t)$ and the resulting signals are $x_{\mathrm{IF\text{-}I}}(t)$ and $x_{\mathrm{IF\text{-}Q}}(t)$. The signals can be represented (Iovescu & Rao, 2016) as:

$$x_{\mathrm{IF-I}}(t) = LPF\{x_{\mathrm{T}}(t) \cdot x_{\mathrm{R}}(t)\} = A_{\mathrm{IF-I}} \cos(2\pi\, f_{\mathrm{IF}}\, t \; + \; \phi_{\mathrm{IF-I}}) + n(t) \tag{5}$$

$$x_{\mathrm{IF-Q}}(t) = A_{\mathrm{IF-Q}} \cos\big(2\pi\, f_{\mathrm{IF}}\, t \; + \; \phi_{\mathrm{IF-Q}}\big) + n(t) \tag{6}$$

where A_{I} and A_{Q} are the amplitude, $\phi_{\mathrm{IF\text{-}I}}$ and $\phi_{\mathrm{IF\text{-}Q}}$ are the phases of the signal $x_{\mathrm{IF\text{-}I}}(t)$ and $x_{\mathrm{IF\text{-}Q}}(t)$, $f_{\mathrm{IF}} = f_{\mathrm{T}}(t)$-$f_{\mathrm{R}}(t)$ is the frequency and is the same for both signals, and $n(t)$ is noise. The f_{IF} is constant in time(Figure 5b) and this frequency is called *beat frequency* (Li et al, 2021). Figure 5 refers to only one chirp and one target.

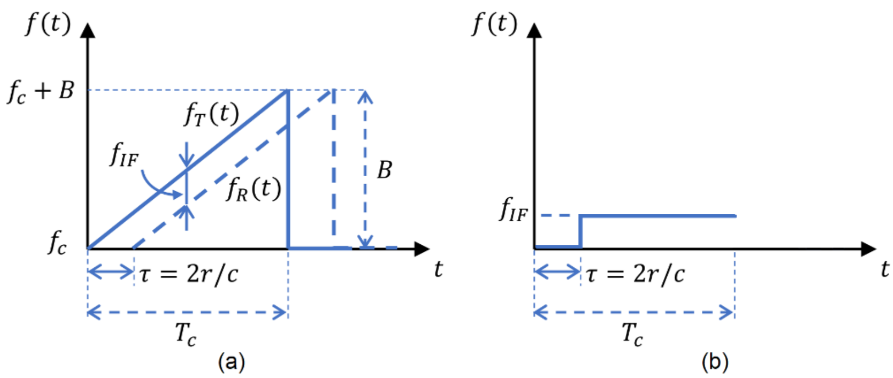

Figure 5 – Frequency of the transmitted and received chirp signal (a), frequency of the signal at the intermediate frequency (b) (Li et al, 2021)

The signals $x_{\mathrm{IF-I}}(t)$ and $x_{\mathrm{IF-Q}}(t)$ are sampled and form the signal $x_{\mathrm{IF}}[n] = x_{\mathrm{IF-I}}[n] + jx_{\mathrm{IF-Q}}[n]$. Viewed in the time domain, it can be observed that a complex exponential IF signal is obtained at the output of the quadrature receiver, which is equal to (Li et al, 2021; Ramasubramanian, 2017):

$$x_{\mathrm{IF}} = A\, e^{j(2\pi\cdot f_{\mathrm{IF}}\cdot t\, +\phi_{\mathrm{IF}})} + n(t)\ , \tag{7}$$

where is the amplitude $A = \sqrt{{A_{\mathrm{IF-I}}}^2 + {A_{\mathrm{IF-Q}}}^2}$, phase $\phi_{\mathrm{IF}} = tan^{-1}(\frac{\phi_{\mathrm{IF-Q}}}{\phi_{\mathrm{IF-I}}})$ and f_{IF} is the frequency of the signal x_{IF}.

The transmission signal is reflected from an object located at a range r and arrives at the receiving antennas with a delay τ , which is calculated as: $\tau = \frac{2r}{c}$, where c is the speed of light, that is the speed of electromagnetic wave propagation. If the target does not move, the frequency of the IF signal remains constant during the reception period, while the transmit and receive chirp signals overlap in time and are equal to: $f_{\mathrm{IF}} = f_{\mathrm{T}}(t)$-$f_{\mathrm{R}}(t) = S\,\tau$.

The phase of the IF signal can be determined at the moment of IF signal onset, when the reflected chirp signal arrives at the receiving antenna. Taking into account expression (3), the phase of the chirp signal is approximately equal to (Li et al, 2021): $\phi_{\mathrm{IF}} \approx 2\pi\, f_{\mathrm{c}}\, \tau$.

It turns out that the frequency and phase of the IF signal, which is received from an object located at a range r, is equal to(Li et al, 2021):

$$f_{\mathrm{IF}} = S\,\tau = \frac{2\,S\,r}{c}, \tag{8}$$

$$\phi_{\mathrm{IF}} = 2\pi\, f_{\mathrm{c}}\, \tau = \frac{4\pi\, r}{\lambda}. \tag{9}$$

When the chirp signal is bounced from multiple targets back to the radar, the received IF signal is a linear combination of multiple IF signals, each with a frequency and phase corresponding to the range of each individual target.

Digital processing of radar signals

This chapter explains the organization of radar data that is suitable for further processing. The standard flow of signal processing is shown and it is explained how to determine the DFT coefficients and thus obtain information about the target.

Radar signal sampling

A radar data cube is a three-dimensional data structure, which is a convenient way to conceptually represent the time-space processing of radar data. This way of organizing data is common to all modern radar systems, whether they are pulsed or continuous radars. The cube of radar data contains three axes and its cells contain the selected values of the reflected IF signal (Figure 6) (MathWorks, 2024). For MIMO radars and virtual antennas, the formation of a unified radar data cube is shown in Figure 11.

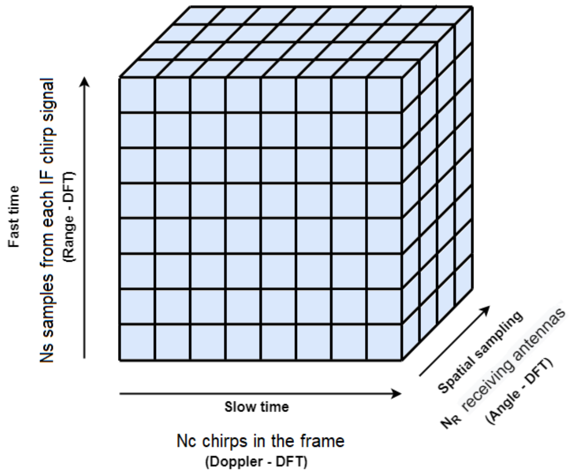

Figure 6 – Radar data cube

In the Fast Time Axis, signal samples are placed within a single chirp, i.e., within the repetition period of the radar signal (pulse) in pulse radars. This axis contains N_S samples, selected at a frequency F_S. The Slow Time Axis contains data from multiple chirp signals, with multiple chirps forming a single frame. In the Spatial Axis, samples of the signal received by all receiving antennas are placed. The spatial axis contains N_R samples, equal to the number of receiving antennas. In the case of MIMO radars, it contains a number of samples equal to the number of virtual receiving antennas (MathWorks, 2024).

The flow of digital radar signal processing

The digital radar signal processing flow includes a series of steps that involve processing the raw radar signal to obtain target information (Figure 7). As the output of the processing, the Range-Velocity and Range-Angle matrices are obtained, which provide all three important pieces of information about the target. Later, the classification and tracking procedure can be entered (Li et al, 2021, p.167967).

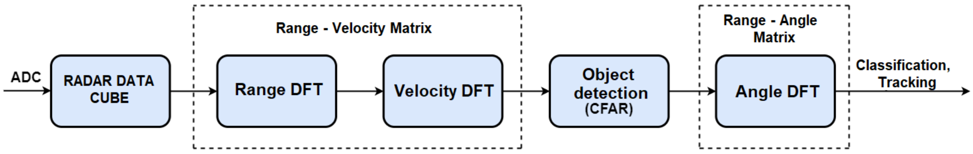

Figure 7 – Flow of digital processing of the radar signal

After AD conversion of the IF signal, the samples are organized into a radar data cube. Radar data cubes are formed, as explained in the chapter above, from samples of signals originating from different transmitting antennas. After organizing the data, the first step is to determine the Range DFT coefficients on each of the sampled IF chirp signals. The range DFT is applied along the columns to all chirps and from all virtual antennas. By applying the Discrete Fourier Transform (DFT) along the fast time axis, the *beat frequency* is observed and information about the distance of the targets is obtained. After the Range DFT, over the already calculated DFT coefficients, the Velocity DFT (Doppler DFT) is applied along all rows within the frames of all receiving virtual antennas. By applying the DFT along the slow time axis, the phase shift caused by the movement of the target is observed, Doppler processing is performed and information on the speed of the target's movement is obtained (Figure 8a). In this paper, all Range – Velocity DFT coefficients were calculated for the matrix representation, but in general, not all coefficients are used. By combining these two DFT algorithms, the Range-Velocity matrix is obtained for all virtual antennas (Li et al, 2021, p.167967).

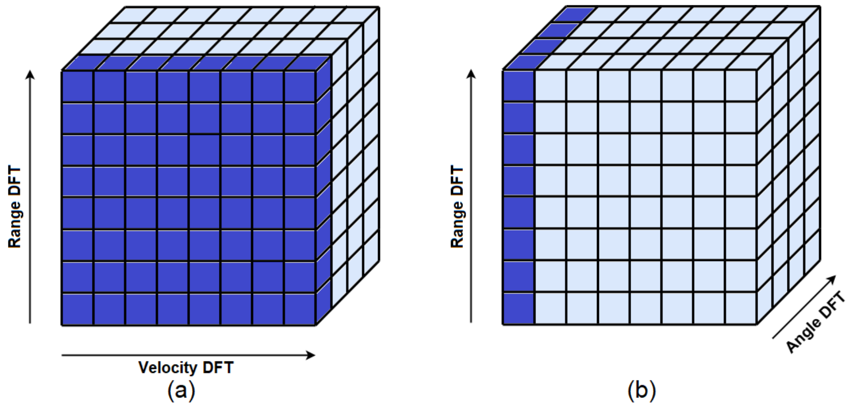

Figure 8 – Range and Velocity DFT (a), Range and Angle DFT (b)

Target detection is performed on the Range-Velocity matrices or CFAR (Constant False Alarm Rate) is applied in order to separate targets from noise. These algorithms are performed on the Range-Velocity matrices of all antennas. All matrices are summed into a single combined Range-Velocity matrix, where even targets with a low SNR (Signal-to-Noise Ratio), which were not detected in all matrices, will be observed.

After the detection of targets, or the application of CFAR and filtering in the frequency domain, the Angle DFT in the third dimension of the radar data cube is applied over the calculated DFT coefficients, over all virtual antennas (Figure 8b). Since the duration of the frame is a few milliseconds, it can be assumed that targets, due to their movement, will not change the resolution cell, and before the Angular DFT, it is not necessary to perform Doppler phase compensation. The Range-Angle matrices are obtained for each of the possible velocity of the targets. Finally, by adding all the amplitude characteristics of the Range-Angle matrices, one unified matrix is obtained that provides information about the distance and the angle at which the target is located. The amplitude characteristics of the matrices are displayed using a two-dimensional heat map or in a three-dimensional display. By observing the maximum of the functions, the distance, velocity, and azimuth of the target are determined (Li et al, 2021, p.167967).

Range DFT

By applying the DFT along the fast time axis, the N_S of the signal samples is obtained. According to the theory of the discrete Fourier transform, each cell of the DFT corresponds to the frequency $f_k = k\frac{f_S}{N_S}$ for $0 \leq k < N_S$. Based on expression (8), which describes the relationship between the *beat frequency* and the distance of the targets, and the calculation of the frequency in the DFT cells, it is concluded that the distance of the targets in relation to the DFT cell is equal to (Li et al, 2021):

$$r_k = f_k \frac{c}{2S} = k\,\frac{cf_S}{2SN_S} \qquad (10)$$

for $0 \leq k < N_S$. By applying the Range DFT, and displaying the amplitude spectrum $|X[k]|$, a peak in the cell is observed on the range and by applying expression (10) the distance to the target corresponding to the reflected signal can be determined (Li et al, 2021).

In this application f_{IF} is positive, due to the assumed signal and system model. The use of a quadrature receiver the spectrum of a complex exponential signal (7) can be observed on the full spectrum from *0* to f_s, by considering the spectrum at negative frequencies, ranging from $-f_s/2$ to 0, as the spectrum at frequencis from $f_s/2$ to f_s. (Ramasubramanian, 2017). In this regard, the maximum distance at which an object can be detected, with the condition that $f_{IF} < f_s$. is equal to (Li et al, 2021, p.167962):

$$r_{max} < \frac{c\, f_s}{2S}. \tag{11}$$

The received signal is a linear combination of several individually reflected signals from objects at different distances. As the DFT is a linear transform, the total signal spectrum is a linear combination of multiple individual spectra from each signal. Targets at different distances will appear in different cells of the spectrum and we can distinguish them if their mutual distance is greater than the resolution cell by the distance r_s. Therefore, the range resolution depends on the frequency detection resolution $f_{\mathrm{res}} = \frac{f_s}{N_s}$, so the range resolution is equal to (Li et al, 2021, p.167962):

$$r_{\mathrm{res}} = f_{\mathrm{res}} \frac{\mathrm{c}}{2S} = \frac{\mathrm{c} f_s}{2SN_s}. \tag{12}$$

Velocity DFT

The radar emits an N_c chirp signal of the duration T_c within the frame duration T_f (Figure 9). In order to measure the velocity of the target's movement, the radar must transmit a minimum of two separate chirp signals within the frame in order to detect the phase change due to the target's movement. If the target is moving at the radial speed v_r, during the time period until the next signal T_c is transmitted, the target travels the distance $\Delta r = v_r \cdot T_c$ (Li et al, 2021, p.167962).

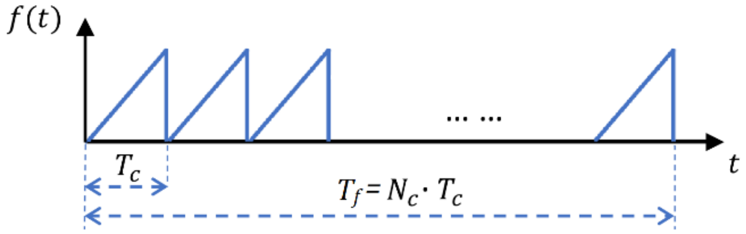

Figure 9 – Transmitted frame of the N_c chirp signal (Li et al, 2021)

The difference in the frequency of the two IF signals is negligible, while based on the signal model (9), the phase difference is equal to (Li et al, 2021):

$$\Delta\phi = \frac{4\pi\Delta r}{\lambda} = \frac{4\pi v_r T_c}{\lambda}. \tag{13}$$

Applying the DFT along the slow time axis gives the target velocity equal to (Li et al, 2021):

$$v_l = \omega_l \frac{\lambda}{4\pi T_\mathrm{c}} = l \frac{\lambda}{2N_\mathrm{c}T_\mathrm{c}} = l \frac{\lambda}{2T_\mathrm{f}}, \tag{14}$$

where $\omega_l = \frac{2\pi l}{N_\mathrm{c}}$, N_c is the number of Velocity DFT samples and $-\frac{N_\mathrm{c}}{2} \leq l < \frac{N_\mathrm{c}}{2}$ assuming that N_c is an even number (Proakis & Manolakis, 2014). T_f is the frame duration or also known as the time on the target.

Unambiguous velocity measurement is performed in the range $-\pi \leq \omega < \pi$, so the unambiguous detectable velocity is equal to (Li et al, 2021):

$$-\frac{\lambda}{4T_\mathrm{c}} \leq v < \frac{\lambda}{4T_\mathrm{c}}, \tag{15}$$

where positive speed means a movement towards from the radar, and a negative movement occurs away from the radar.

The velocity resolution is equal to one resolution cell and amounts to (Li et al, 2021):

$$v_\mathrm{res} = \frac{\lambda}{2N_\mathrm{c}T_\mathrm{c}} = \frac{\lambda}{2T_\mathrm{f}}. \tag{16}$$

It is concluded that the longer the frame, the better the separation of two targets with similar velocity, with the condition that the target does not move to another resolution cell during that time.

Angle DFT

By using an array of receiving antennas, the angle of arrival of the echo signal can be estimated. The echo wave arrives at a certain angle to the receiving array and due to the mutual distance between the receiving antennas, a relative signal delay occurs between the two receiving antennas. Signal delay is reflected in the change in frequency and phase of the IF signal. The frequency change is negligibly small while the phase shift is equal to (Li et al, 2021):

$$\Delta\phi = 2\pi\, f_\mathrm{c}\, \Delta\tau = \frac{2\pi\, d\, sin(\Theta)}{\lambda}, \tag{17}$$

where $\Delta\tau$ is the signal delay, due to the spacing between the receiver antennas and it is equal $\Delta\tau = d \sin(\Theta)\, /c$ (Figure 2).

Applying the DFT to all antennas results in the angle under which the target is located being equal to (Li et al, 2021):

$$\Theta u \; = \; sin^{-1}(\omega_u \frac{\lambda}{2\pi d}) \; = sin^{-1}(u \frac{\lambda}{Nd}), \tag{18}$$

where $\omega_u = \frac{2\pi u}{N}$ (Proakis & Manolakis, 2014), *N* is the number of Angle DFT samples, $-\frac{N}{2} \leq u < \frac{N}{2}$, assuming that *N* is an even number and *d* is the distance between the receiving antennas.
An unambiguous estimate of the angle can be determined in the range:

$$-sin^{-1}(\frac{\lambda}{2d}) \leq \theta < sin^{-1}(\frac{\lambda}{2d}). \tag{19}$$

In real applications, the distance between the antennas is often taken as the value $d = \frac{\lambda}{2}$, which corresponds to the fact that the angle can be estimated in the range $-90º \leq \theta < 90º$, where θ is defined in relation to broadside.

The angular resolution θ_{res} depends on the number of N_R receiving antennas and the central viewing angle of the target $\tilde{\theta}$ and is equal to (Li et al, 2021):

$$\theta res = |\Delta\theta| = 2 \cdot sin^{-1}(\frac{\lambda}{2N_R d\, cos(\tilde{\theta})}). \tag{20}$$

Assuming that $\tilde{\theta} = 0$ and $d = \frac{\lambda}{2}$, a rough estimate of the angular resolution is obtained, which is equal to (Li et al, 2021):

$$\theta res = \frac{2}{N_R}. \tag{21}$$

Improvement of angular resolution using the MIMO mode

A MIMO radar system has an antenna arrangement as shown in Figure 2 and by using the MIMO mode, virtual antennas are formed. By increasing the number of antennas, the angular resolution also improves. As the radar system works on the principle of time-multiplexed transmission signals, it first emits signals from one transmitter, and then from the other transmitter antenna (Figure 10). In this way, two radar data cubes are formed at reception (Li et al, 2021, p.167966).

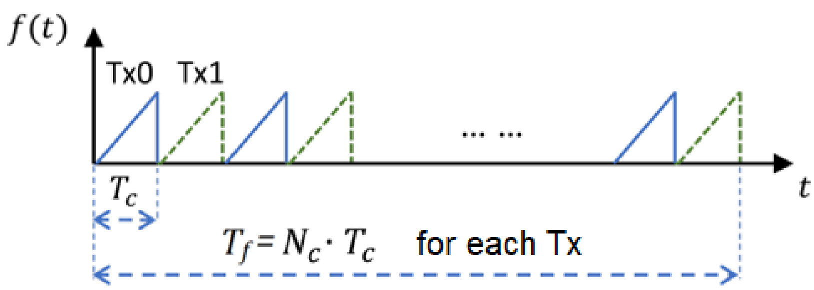

Figure 10 – Chirp signal frame with two transmitting MIMO antennas (Li et al, 2021)

Radar data cubes are formed for signals transmitted from different transmitting antennas. Since the condition of the distance between transmitting antennas in MIMO radars is met, a unified radar data cube (Figure 11) can be formed, which will have the properties as if there were 8 receiving antennas sent from one transmitting antenna.

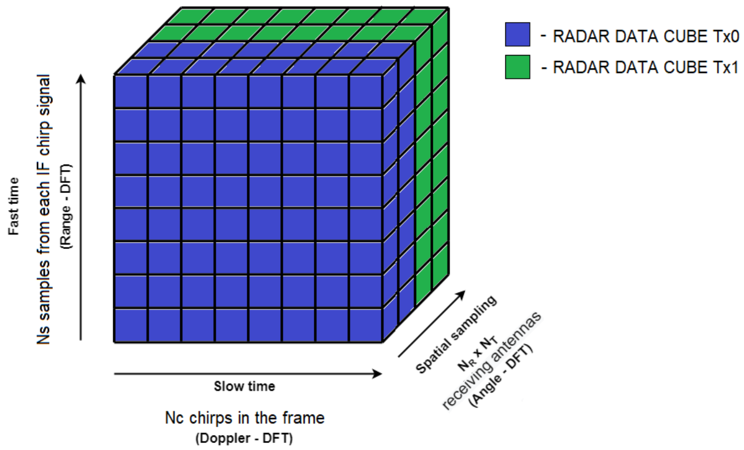

Figure 11 – Unified radar data cube

Simulation of a MIMO radar system

The Matlab functions for generating simulation and automated processing of the radar data cube are explained below. Te radar and target parameters for simulation purposes are defined and the simulation results are presented.

Generation of simulation echo signals of radar targets

In order to confirm the analytical claims in this paper, computer simulations were developed in the Matlab programming environment. The MIMOFMCW function was developed for simulation purposes. The mentioned function generates IF samples of the reception signal (7) that originated from the targets and were sent from one transmitting antenna. The output parameter is a three-dimensional radar data cube.

Processing of simulation radar data

In order to automate the process of digital processing of radar data, the procDC function was developed. The outputs of the function are two two-dimensional matrices RV - Range-Velocity matrix and RA - Range-Angle matrix. In addition to the matrices as an output, the function in the command window prints the range of unique measurement of the range, velocity and angle of the radar for the given parameters and displays two three-dimensional views of the specified matrices with normalized axes, normalized in relation to the maximum value that appears in the matrix.

Simulation - Situation 1

The objective of situation 1 is to demonstrate the general operation of the radar for arbitrary parameters of the radar and targets. Table 1 shows the radar parameters adjusted for situation 1.

Table 1 – Simulation radar parameters - Situation 1

N_o	512	B	1 GHz
N_c	256	S	10 GHz/ms
T_c	0.1 ms	N_{Tx}	2
T_f	25.6 ms	N_{Rx}	4
f_s	5.12 MHz	d_{Rx}	$\lambda/2$
f_c	24 GHz	d_{Tx}	$4 \cdot d_{Rx}$

With the given parameters from Table 1, the radar achieves an unambiguous range of 76.80 m (11), unique speed measurement in the range from -31.25 m/s to 31.25 m/s (15) and the angle estimation from -90º to 90º (19). The distance between the transmitting antennas is satisfactory and allows the radar to work in the MIMO mode and behave as if it has 8 instead of 4 receiving antennas. In Table 2, the goal parameters adjusted for situation 1 are given.

Table 2 – Parameters of simulation targets - Situation 1

No	***A* (V)**	***r* (m)**	***v* (m/s)**	**θ (º)**
1	1	70	-28	60
2	0.9	55	20	-30
3	0.85	40	-15	45
4	0.7	35	10	-45
5	0.6	20	5	0

Figure 12 shows the Range-Velocity matrix related to situation 1. In the image, peaks can be clearly observed, which correspond to the parameters set by the targets.

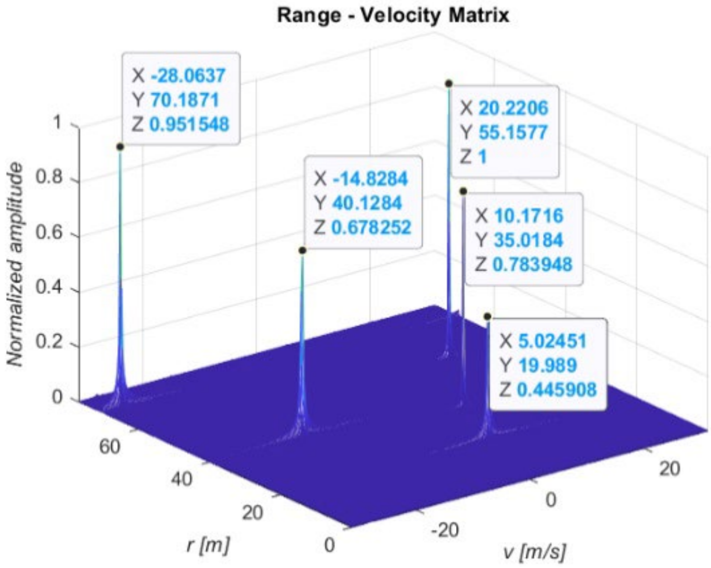

Figure 12 – Range-Velocity simulation matrix - Situation 1

In Figure 13a), the Range-Angle matrix is shown, simulating the operation of 1 transmitting and 4 receiving antennas. The radar data cube is padded along the angular axis with zeros to calculate the Angle DFT in 128 points. Zero-padding does not improve resolution but makes the signal spectrum more noticeable and easier to interpret. It can be concluded that due to the small number of receiving antennas, the angular resolution of the cell is considerable and that it is not possible to precisely determine the angle at which the target is in relation to the radar. Limited angular resolution causes a wide main lobe, but by finding the maximum values in the main lobes, one can come to the conclusion at which angle the target is located, but with a decision error. Also, due to the small angular resolution, the main lobes of the targets located at large angles are mirrored from one part of the range to another.

In Figure 13b), the Range-Angle matrix using 2 transmitting and 4 receiving antennas in the MIMO radar mode is shown. In this way, the effect is obtained as if there are 8 receiving antennas, which increases the angular resolution of the radar and narrows the main lobe. In this way, the error when measuring the angle is not drastically reduced, but it enables better separation of two close targets located at similar distances and at similar angles. It also reduces the aliasing effect. Using a single transmitting antenna gives the FWHP of 53.86º, while using the MIMO mode gives the FWHP (Full Width at Half Power) of 27.14º.

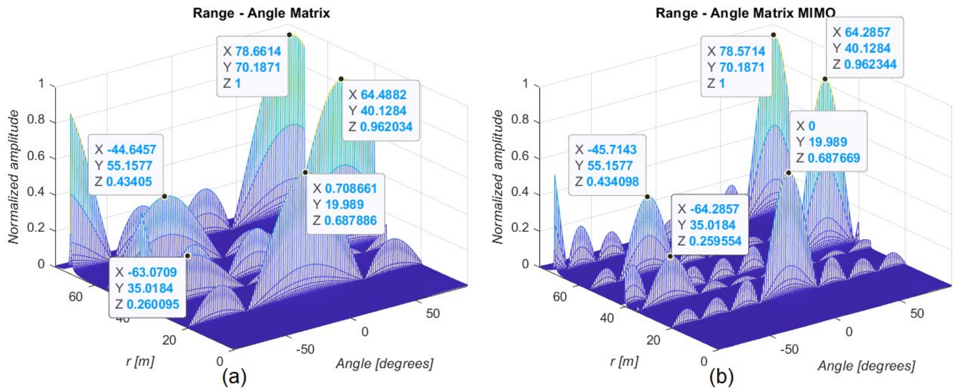

Figure 13 – Range-Angle simulation matrices - Situation 1, 1 Tx, 4 Rx (a); 2 Tx, 4 Rx (b)

Simulation - Situation 2

The purpose of simulation 2 is to show the angular resolution of the radar system and the improvement of the angular resolution using multiple transmit antennas, i.e., the MIMO mode of operation. Also, unlike simulation 1, which is shown under ideal conditions, simulation 2 includes noise where the SNR is -5 dB. Table 3 shows the parameters of the radar system for situation 2.

Table 3 – Simulation radar parameters - Situation 2

N_o	32	B	1 GHz
N_c	128	S	2 GHz/ms
T_c	0.5 ms	N_{Tx}	2
T_f	64 ms	N_{Rx}	4
f_s	64 KHz	d_{Rx}	$\lambda/2$
f_c	24 GHz	d_{Tx}	$4 \cdot d_{Rx}$

According to the parameters listed in Table 3, the radar has the following characteristics: the maximum unique range of 4.80 m; the unambiguous speed measurement range from -6.25 m/s to 6.25 m/s; and the angle measurement range from -90º to 90º with an angular resolution of 28.65º when using one transmitting antenna, or 14.32º when using two transmitting antennas.

Table 4 gives the parameters of the targets adjusted for situation 2. The targets are arranged in pairs to show the effect of separating the targets by angle. Targets one and two are at the same distance, moving at the same speed, but at different angles from the radar. Targets two and three are at the same distance, but moving at different speeds and at different angles, clustered around 0º. For objectives five and six, similar conditions apply to the previous two objectives, except that they are grouped around 60º.

Table 4 – Parameters of simulation targets - Situation 2

No	*A* (V)	*r* (m)	*v* (m/s)	*θ* (º)
1	1	4,3	5	-40
2	0.9	4,3	5	30
3	0.8	2.5	-3	-10
4	0.8	2.5	4	10
5	0.6	0,5	-1	50
6	0.6	0,5	2	70

In Figure 14, one can see the Range-Velocity matrix related to situation 2. The Figure shows five peaks corresponding to five targets, although six targets are set in the simulation. Targets number one and two are located at the same distances and move at the same speeds, so they cannot be separated on the Range-Velocity matrix, while the other targets are clearly visible.

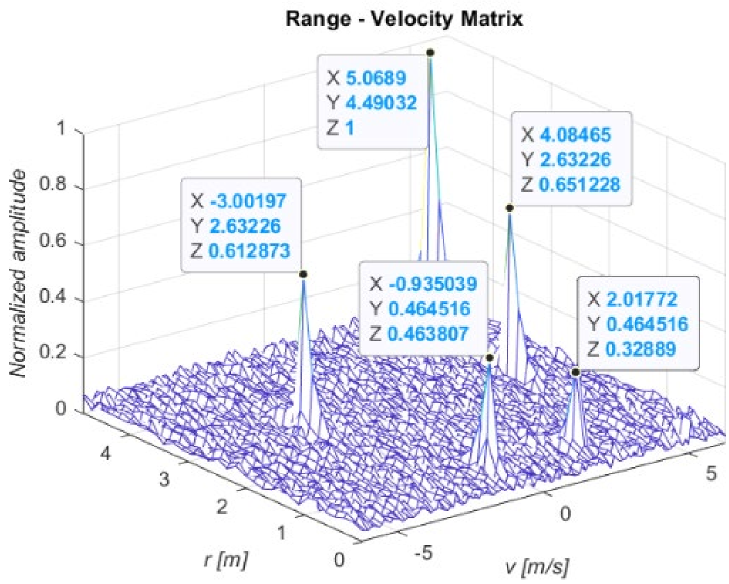

Figure 14 – Range-Velocity simulation matrices - Situation 2

In Figure 15a), there is a Range-Angle matrix that corresponds to the use of one transmitting and four receiving antennas. Although targets one and two are joined on the Range-Velocity matrix, it is observed that on the Range-Angle matrix the targets can be separated because they are at different angles. Targets three and four, as well as five and six are connected to each other and are located under one lobe. It cannot be concluded whether there is one or two targets. This happens because the angular distance between the targets is equal to 20º, and the angular resolution in this mode of operation is equal to 28.65º, and the targets are located in one resolution cell.

In Figure 15b), the Range-Angle matrix is shown when the radar is operating in the MIMO mode, where it uses two transmitting and four receiving antennas and forms a virtual antenna array on reception of eight receiving antennas. In this way, it increases the angular resolution and reduces the resolution cell to 14.32º (21). Targets three and four can be separated, while targets five and six remain under one main lobe - they cannot be separated even though they are at the same angular distance from each other as targets three and four.

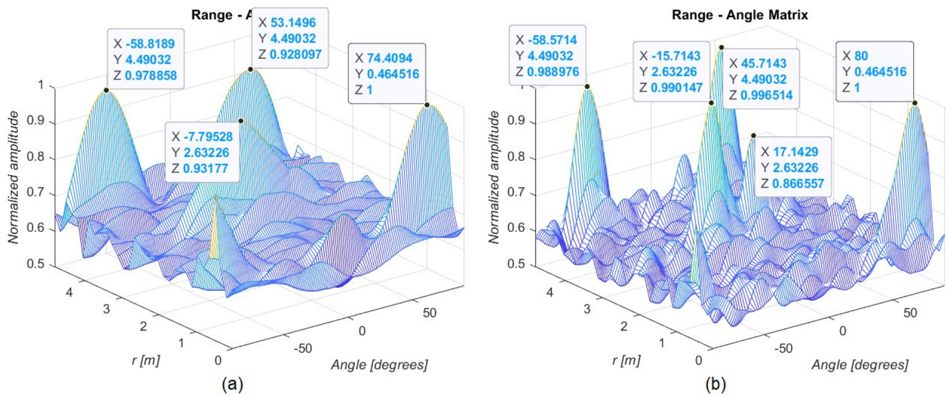

Figure 15 – Range-Angle simulation matrices - Situation 2, 1 Tx, 4 Rx (a); 2 Tx, 4 Rx (b)

It is observed that with the increase of the viewing angle, the angular resolution decreases, that is, the cell resolution increases, which leads to the fact that targets five and six cannot be separated angularly. Figure 16 shows the angular resolution for eight receiving antennas and an observation angle of 60º equal to 28.95º, which explains why targets five and six are not separated on the Range-Angle matrix.

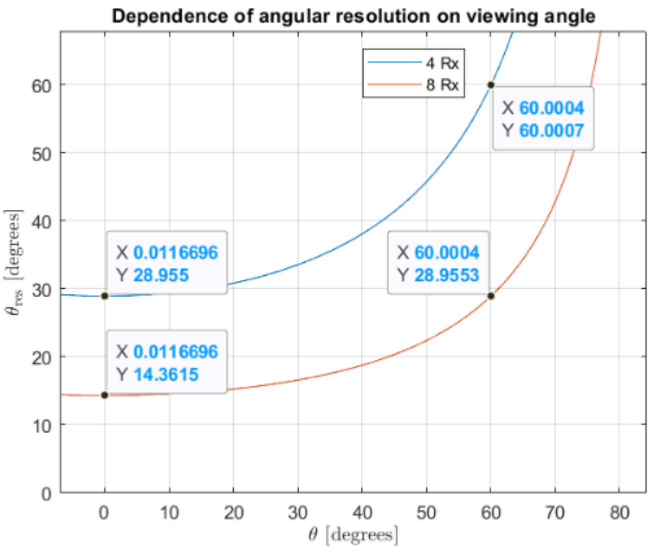

Figure 16 – Dependence of angular resolution on a viewing angle for 4 and 8 receiving antennas

Experimental verification of the MIMO radar model

During the experimental work, the MIMO radar platform PUP_DUAL24P_T2R4 (Figure 17a) from Luswave Technology (2020) was used. The radar platform operates in the K band and supports the continuous operation mode and th eFMCW modulation. The radar has two transmitting and four receiving antennas which enable the MIMO mode of operation and the creation of eight virtual antennas, resulting in a better angular resolution. In addition to the MIMO operating mode, the radar has the option of using only one transmitting antenna which behaves like a conventional radar. The radar comes with a Matlab graphical interface that allows setting the parameters of the radar. The parameters that can be adjusted are the number of transmitting and receiving antennas, the type of modulation, the operating frequency range, the duration of the chirp, the number of selections in the chirp and the length of data recording (Figure 17b) (Luswave, 2020).

The aforementioned radar from which the data was recorded onto the computer (Figure 18) was used in the experimental work. Through the computer, the parameters of the radar were set depending on the situation. The computer was later used to process and display the recorded data.

Specification	Minimum	Typical	Maximum
Channels		2x Transmitters, 4x Receivers	
Antennas		6x Onboard Patch Antennas	
Modulations		FMCW, CW	
Typical Frequency Range	24GHz		25GHz
Expandable Frequency Range	23.5GHz		26GHz
Sweep Time		0.5ms, 1ms, 2ms, 4ms, 8ms	
Samples per Sweep		128, 256, 512, 1024, 2048, 4096	
Tune Voltage	0		4V
Tuning Sensitivity		0.8GHz/V	
Transmit Power	16dBm	17dBm	18dBm
SSB Phase Noise @1MHz offset		-99dBc	
Noise Figure		12dB	
Maximum Input Power		5dBm	
IIP_1dB		-12dBm	
Supply Voltage	5.75V	6V	6.25V
Supply Current		1200mA	
Operating Tempreture	-40°C		85°C
Dimensions		L:130mm, W:108mm, H:32mm	

(a) (b)

Figure 17 – MIMO radar PUP_DUAL24P_T2R4 (a); Radar specifications (b) (Luswave, 2020)

Figure 18 – Radar and computer used for experimental imaging

For the purpose of the experiment, the recorded situations were those in which a person moves to and from the radar, to the left and to the right, while changing the speed of movement and the angle at which one is in relation to the radar (Figure 19a).

The person holds a reflector ball in the hands (Lunenberg lens) in order to increase the reflection and thus make the results more noticeable (Figure 19b).

(a) (b)

Figure 19 – Man as a radar target (a); Radar reflector (Lunenberg lens) (b)

Experiment - Situation 1

For the purpose of experimental verification, the radar parameters listed in Table 5 were used. According to the listed parameters, the radar has the following characteristics: the maximum unique range of 4.80 m; the unambiguous speed measurement range from -6.25 m/s to 6.25 m/s; and the angle measurement range from -90º to 90º with an angular resolution of 28.65º when using one transmitting antenna, or 14.32º when using two transmitting antennas.

Table 5 – Radar parameters of the experiment - Situation 1,2

N_o	32	f_c	24 GHz
N_c	128	B	1 GHz
T_c	0.5 ms	S	2 GHz/ms
T_f	64 ms	N_{Tx}	2
f_s	64 KHz	N_{Rx}	4

For situation 1 of the experiment, the person moves away from the radar from the right side of the radar. Figure 20 shows the Range-Velocity matrix of the experiment, where one intense peak is observed, which corresponds to the target. By reading the peak value, information is obtained about the distance and speed of the target.

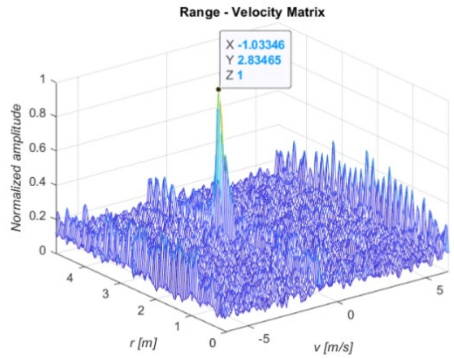

Figure 20 – Range- Velocity matrix of the experiment - Situation 1

When processing the data and displaying the Range-Velocity matrix, it is observed that the matrix contains unwanted components and a high level of noise. In order to reduce the influence of noise and make the results more obvious, before applying the Angle DFT algorithm, the observed object of interest is extracted using a 3x3 unit mask, in the center of which the object of interest is located. After the extraction of the object, the values in the matrix will remain only in the cells where the object is located, while the other cells will have a value of zero.

On the Range-Angle matrix, the main lobe is observed, and the search for its maximum determines the angle at which the target is located (Figure 21a). Using two transmitting antennas narrows the main lobe, which increases the angular resolution (Figure 21b). It is observed that the components at all other distances are suppressed, which is the result of extracting the object of importance by using a mask.

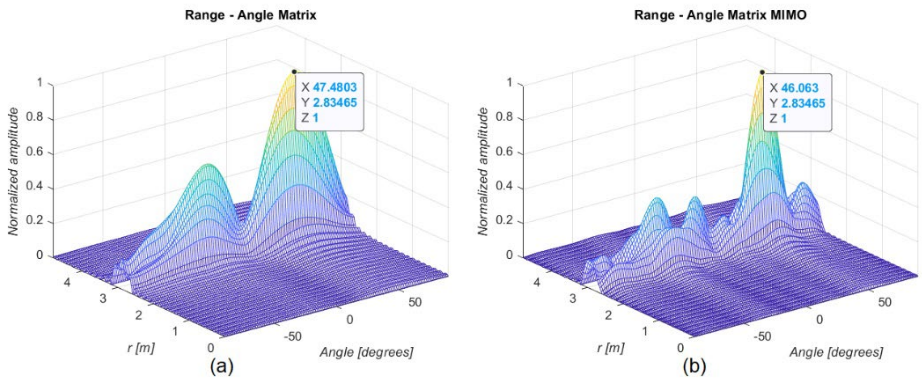

Figure 21 – Range-Angle matrices of the experiment - Situation 1, 1 Tx 4 Rx (a), 2 Tx4 Rx MIMO (b)

Experiment - Situation 2

For situation 2 of the experiment, the same radar parameters as those listed in Table 5 were used. Two people move away from the radar, from the same side and at similar angles (Figure 22).

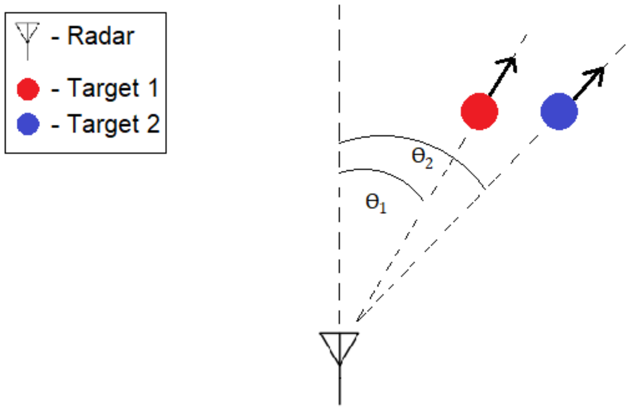

Figure 22 – Approximate sketch of the experiment situation 2

The aim of this experiment is to show better angular resolution using the MIMO mode and to confirm the claims shown in the simulation. By processing the signal, filtering and extracting the objects of interest, two peaks corresponding to two targets are observed, but it is difficult to separate them due to almost the same speed and mode of movement (Figure 23).

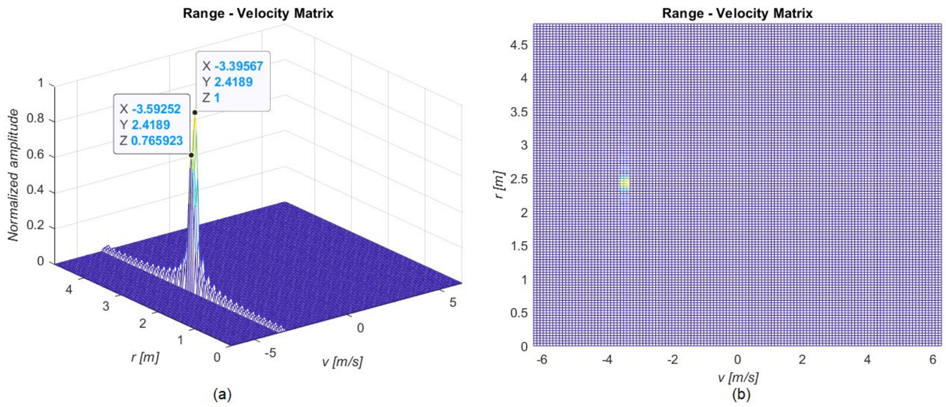

Figure 23 – Range-Velocity matrices of the experiment - Situation 2, 3D view (a), 2D heat map (b)

Since one transmitting and four receiving antennas are used and due to a small angular resolution and a large viewing angle, it is not possible to separate the targets which are both under a wide main lobe. The FWHP is 55.28º, which would lead to a wrong assessment of the situation (Figure 24a). By using two transmitting antennas in the MIMO mode of operation, the angular resolution is increased and is less than 34º. Two main lobes corresponding to the targets are distinguished, where the first FWHP is 25.51º and the second one is 22.68º (Figure 24b). By using an adequate decision-making threshold, a correct conclusion about the situation can be made.

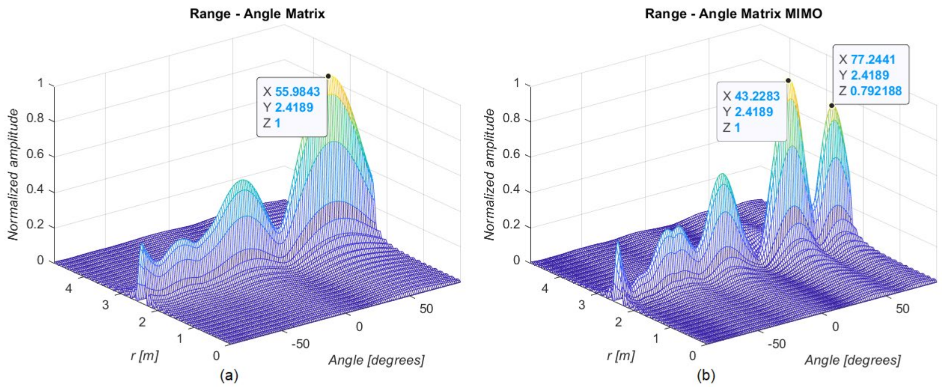

Figure 24 – Range-Angle matrices, - Situation 2, 1 Tx 4 Rx (a), 2 Tx 4 Rx MIMO (b)

Conclusion

In this paper, a model of an FMCW MIMO radar with time-multiplexed signals on transmission is presented, and the process of digital signal processing in this radar type, which primarily utilizes the Discrete Fourier Transform, is explained. The Discrete Fourier Transform has proven to be a straightforward tool that delivers satisfactory results. The theoretical foundations and mathematical models have been validated through simulation and experimental verification.

The resolution in the domains of range, velocity, and angle is limited by the use of the DFT algorithm. FMCW radars have been shown to provide accuracy in determining the range and velocity of targets, with the range resolution dependent on the signal sampling frequency f_S, the ramp slope coefficient S and the number of samples per chirp N_S, while the velocity resolution depends on the frame duration T_f. Since the angular resolution depends on the number of receiving antennas, it has been demonstrated that by introducing additional transmitting antennas, forming

VOJNOTEHNIČKI GLASNIK / MILITARY TECHNICAL COURIER, 2025, Vol. 73, Issue 2

a virtual receiving array, and operating the radar in the MIMO mode, the angular resolution and the ability to distinguish targets with similar angles are improved, as illustrated through simulations and experiments. In addition to the above, due to the limited number of receiving antennas, the DFT algorithm is characterized by wide main lobes. The algorithm determines the target angle, albeit with a certain error.

In this study, CFAR was not used, as target detection was trivial and performed manually. In this regard, the system can be improved by introducing an appropriate CFAR model which would automate the detection process. Future research will focus on the development and application of suitable algorithms for more precise target angle determination, such as MUSIC, Decorrelation Algorithms, and Spatial Smoothing. Additionally, research could be expanded to the design and implementation of planar MIMO radar structures, enabling target angle detection in both azimuth and elevation.

References

Abdi, A.H. & Rasheed, H. 2022. Performance Analysis of Outdoor Massive MIMO on Ultra-High Frequency Bands (73 GHz and 100 GHz). In: *2022 International Symposium on Networks, Computers and Communications (ISNCC),* Shenzhen, China, pp.1-6, July 19-22. Available at: https://doi.org/10.1109/ISNCC55209.2022.9851799.

Alizadeh, M., Shaker, G., De Almeida, J.C.M., Morita, P.P. & Safavi-Naeini, S. 2019. Remote Monitoring of Human Vital Signs Using mm-Wave FMCW Radar. *IEEE Access*, *7*, pp.54958-54968. Available at: https://doi.org/10.1109/ACCESS.2019.2912956.

Bliss, D.W. & Forsythe, K.W. 2006. MIMO Radar Medical Imaging: Self-Interference Mitigation for Breast Tumor Detection. In: *2006 Fortieth Asilomar Conference on Signals, Systems and Computers*, Pacific Grove, CA, USA, pp.1558-1562, October 29-November 01. Available at: https://doi.org/10.1109/ACSSC.2006.355020.

Davis, M.S., Showman, G.A. & Lanterman, A.D. 2014. Coherent MIMO radar: The phased array and orthogonal waveforms. *IEEE Aerospace and Electronic Systems Magazine*, 29(8), pp.76-91. Available at: https://doi.org/10.1109/MAES.2014.130148.

Dessai, S.N. & Patidar, H. 2024. Hardware software SoC co-design analysis and implementation of MIMO-OFDM for 4G/5G/6G eNodeB applications. *Transactions on Emerging Telecommunications Technologies*, 35(7), e5012. Available at: https://doi.org/10.1002/ett.5012.

Han, K., Bauduin, M., & Bourdoux, A. 2024. Beamspace Matrix Completion in Subarray-Based Sparse Linear Array for High-Resolution Automotive MIMO Radar. In: *2024 IEEE Radar Conference (RadarConf24)*, Denver, CO, USA, pp.1-6, May 06-10. Available at: https://doi.org/10.1109/RadarConf2458775.2024.10549360.

He, H., Stoica, P. & Li, J. 2009. Designing Unimodular Sequence Sets With Good Correlations—Including an Application to MIMO Radar. *IEEE Transactions on Signal Processing*, 57(11), pp.4391-4405. Available at: https://doi.org/10.1109/tsp.2009.2025108.

Iovescu, C. & Rao, S. 2016. The fundamentals of millimeter wave sensors. *Texas Instruments* [online]. Available at: https://www.ti.com/lit/wp/spyy005a/spyy005a.pdf?ts=1736646797336 [Accessed: 10 May 2024].

Janoudi, V., Schoeder, P., Grebner, T., Schwarz, D., Waldschmidt, C., Dickmann, J. & Appenrodt, N. 2023. Antenna Array Design for Coherent MIMO Radar Networks. In: *2023 IEEE Radar Conference (RadarConf23)*, San Antonio, TX, USA, pp.1-6, May 01-05. Available at: https://doi.org/10.1109/RadarConf2351548.2023.10149789.

Li, X., Wang, X., Yang, Q. & Fu, S. 2021. Signal Processing for TDM MIMO FMCW Millimeter-Wave Radar Sensors. *IEEE Access*, 9, pp.167959-167971. Available at: https://doi.org/10.1109/ACCESS.2021.3137387.

Liu, B. 2009. Orthogonal Discrete Frequency-Coding Waveform Set Design with Minimized Autocorrelation Sidelobes. *IEEE Transactions on Aerospace and Electronic Systems*, 45(4), pp.1650-1657. Available at: https://doi.org/10.1109/taes.2009.5310326.

-Luswave Technology. 2020. *PUP_DUAL24P_T2R4 Datasheet* [online]. Available at: https://luswave.com/PUP_EN24P_T2R4 [Accessed: 1 June 2024].

Mahafza, B.R. 2013. *Radar Systems Analysis and Design using MATLAB*, 2nd Edition. New York: Chapman and Hall/CRC. Available at: https://doi.org/10.1201/9781420057072.

-MathWorks. 2024. *Radar Data Cube* [online]. Available at: https://www.mathworks.com/help/phased/gs/radar-data-cube.html [Accessed: 24 May 2024].

Omer, A.E., Shaker, G., Safavi-Naeini, S., Murray, K. & Hughson, R. 2018. Glucose Levels Detection Using mm-Wave Radar. *IEEE Sensors Letters*, 2(3), pp.1-4. Available at: https://doi.org/10.1109/LSENS.2018.2865165.

Proakis, J.G. & Manolakis, D.G. 2014. *Digital Signal Processing, Fourth Edition*. Harlow, Essex, UK: Pearson. ISBN: 978-1-292-02573-5.

Ramasubramanian, K. 2017. Using a complex-baseband architecture in FMCW radar systems. *Texas Instruments* [online]. Available at: https://www.ti.com/lit/wp/spyy007/spyy007.pdf [Accessed: 5 May 2024].

Rao, S. 2018. MIMO Radar. *Texas Instruments*, July [online]. Available at: https://www.ti.com/lit/an/swra554a/swra554a.pdf?ts=1736649852855 [Accessed: 3 May 2024].

Richards, M.A. 2014. *Fundamentals of Radar Signal Processing, 2nd Edition.* New York: McGraw-Hill Education [online]. Available at: https://www.accessengineeringlibrary.com/content/book/9780071798327 [Accessed: 3 May 2024]. ISBN: 9780071798327.

Stoica, P. & Li, J. 2008. *MIMO Radar Signal Processing*. John Wiley & Sons, Inc. Available at: https://doi.org/10.1002/9780470391488.

Sun, H. 2023. Introduction to MIMO Radar Waveforms. *IEEE AESS,* 13 April [online]. Available at: https://ieee-aess.org/presentation/lecture/introduction-mimo-radar-waveforms [Accessed: 25 April 2024].

Sun, H., Brigui, F. & Lesturgie, M. 2014. Analysis and comparison of MIMO radar waveforms. In: *2014 International Radar Conference,* Lille, France, pp.1-6, October 13-17. Available at: https://doi.org/10.1109/radar.2014.7060251.

Wang, Z., Shi, D. & Wu, H. 2021. The Role of Massive MIMO and Intelligent Reflecting Surface in 5G/6G Networks. In: *2021 International Conference on Wireless Communications and Smart Grid (ICWCSG)*, Hangzhou, China, pp.309-312, August 13-15. Available at: https://doi.org/10.1109/ICWCSG53609.2021.00067.

Wiesbeck, W., Sit, L., Younis, M., Rommel, T., Krieger, G. & Moreira, A. 2015. Radar 2020: The future of radar systems. In: *2015 IEEE International Geoscience and Remote Sensing Symposium (IGARSS),* Milan, Italy, pp.188-191, July 26-31. Available at: https://doi.org/10.1109/igarss.2015.7325731.

Wu, C., Zhang, Z., Chen, L. & Yu, W. 2019. The Same Range Line Cells Based Fast Two-Dimensional Compressive Sensing For Airborne MIMO Array SAR 3-D Imaging. In: *IGARSS 2019 - 2019 IEEE International Geoscience and Remote Sensing Symposium*, Yokohama, Japan, pp.3653-3656, July 28-August 02. Available at: https://doi.org/10.1109/IGARSS.2019.8900050.

Procesamiento de señales digitales en radares MIMO con señales de transmisión multiplexadas en el tiempo

Borko B. Đaković[a], *Slobodan* M. Simić[b],
Lidija M. Trivundža[c], *Aleksandar* G. Ristić[d]

[a] Fuerzas Armadas de Serbia, Estado Mayor,
Dirección de Telecomunicaciones y Tecnologías de la Información (J-6),
Centro de Matemáticas Aplicadas y Electrónica,
Belgrado, República de Serbia, **autor de correspondencia**

[b] Universidad de Defensa de Belgrado, Academia Militar,
Departamento de Sistemas Electrónicos Militares,
Belgrado, República de Serbia

[c] Fuerzas Armadas de Serbia, Estado Mayor,
Dirección de Desarrollo y Equipamiento (J-5),
Centro de pruebas técnicas, Belgrado, República de Serbia,

[d] Ministerio de Defensa de la República de Serbia,
Instituto Técnico Militar, Belgrado, República de Serbia

CAMPO: procesamiento de señales digitales, telecomunicaciones, electrónica, electromagnética
TIPO DE ARTÍCULO: artículo científico original

Resumen:

Introducción/objetivo: Un tema actual de importantes esfuerzos de investigación y desarrollo en el campo de los sistemas de radar es la tecnología de radar MIMO (múltiple entrada-múltiple salida). Los radares MIMO representan un avance revolucionario en la tecnología de radar, ya que el uso de múltiples antenas transmisoras que emiten formas de onda ortogonales permite una mejor detección y resolución angular. Para lograr resultados efectivos, el procesamiento de señales digitales de alta calidad y la aplicación de algoritmos avanzados son esenciales para obtener información del objetivo. Este artículo pone especial énfasis en los radares MIMO coherentes, con el objetivo de mejorar la resolución angular. La multiplexación en el tiempo de las señales de transmisión se aplica como método principal para lograr la ortogonalidad entre señales, utilizando una señal de onda continua de frecuencia modulada (FMCW) como base para la forma de onda de transmisión. El objetivo de este artículo es proporcionar y explicar los fundamentos del procesamiento digital de señales en radares MIMO, presentar expresiones analíticas y validarlas mediante simulación y verificación experimental.

Métodos: Se presentan los fundamentos teóricos, utilizando la Transformada Discreta de Fourier (DFT) como herramienta principal en el procesamiento de señales digitales para obtener información sobre la distancia, velocidad y azimut del objetivo. Se desarrolló una simulación en el paquete de software MATLAB para analizar el desempeño del modelo del sistema radar. Se realizó una verificación experimental, donde se registraron escenarios específicos utilizando la plataforma de radar PUP_DUAL24P_T2R4 y posteriormente se procesaron los datos recopilados. Las funciones de MATLAB MIMOFMCW y procDC se escribieron para generar muestras de simulación de señales de eco y para automatizar el procesamiento de señales y la visualización de matrices características de rango-velocidad y rango-ángulo.

Resultados: La simulación y la verificación experimental confirman la validez de los fundamentos teóricos relacionados con el procesamiento de señales digitales en radares MIMO, y los parámetros objetivo se pueden determinar claramente.

Conclusión: La Transformada Discreta de Fourier es una herramienta sencilla que proporciona resultados satisfactorios para determinar el alcance, la velocidad y el ángulo de los objetivos. Los radares FMCW ofrecen precisión para determinar el alcance y la velocidad, mientras que el modo MIMO mejora la resolución angular. El algoritmo DFT es capaz de determinar el ángulo objetivo, pero con un cierto error, lo que hace *necesario el uso de métodos de alta resolución para una determinación más precisa del ángulo.*

Palabras claves: MIMO, radar, TDM, FMCW, cubo de datos de radar, DFT, frecuencia de pulsación, antena virtual.

Цифровая обработка сигналов в радарах MIMO с мультиплексированием по времени сигналов передачи

Борко Б. Джакович[а], *Слободан* М. Симич[б], *Лидия* М. Тривунджа[в], *Александар* Г. Ристич[г]

[а] Вооруженные силы Республики Сербия, Генеральный штаб, Управление телекоммуникаций и информационных технологий (J-6), Центр прикладной математики и электроники, г. Белград, Республика Сербия, **корреспондент**

[б] Университет обороны, Военная академия, кафедра военных электронных систем, г. Белград, Республика Сербия

[в] Вооруженные силы Республики Сербия, Генеральный штаб, Управление развития и оснащения (J-5), Центр технических испытаний, г. Белград, Республика Сербия

[г] Министерство обороны Республики Сербия, Военно-технический институт , г. Белград, Республика Сербия

РУБРИКА ГРНТИ: 47.05.17 Методы приема и обработки сигналов,
47.49.29 Радиолокационные системы, станции,
47.47.29 Радиопередающие устройства,
47.47.31 Радиоприемные устройства,
78.25.00 Вооружение и военная техника,
78.21.49 Военная электроника и кибернетика
ВИД СТАТЬИ: оригинальная научная статья

Резюме:

Актуальной темой важных исследований и разработок в области радиолокационных систем является радиолокационная технология MIMO (множественный вход-множественный выход). Радары MIMO представляют собой революционный прогресс в радиолокационной технологии, поскольку использование нескольких передающих антенн, излучающих ортогональные сигналы, позволяет улучшить обнаружение и угловое разрешение. Для достижения эффективных результатов необходимы качественная цифровая обработка сигналов и применение передовых алгоритмов получения целевой информации. В данной статье особое внимание уделяется когерентным MIMO-радарам с целью улучшения углового разрешения. Временное мультиплексирование сигналов передачи применяется в качестве основного метода *достижения ортогонализации между сигналами с использованием сигнала непрерывной волны с частотной модуляцией (FMCW) в качестве основы формирования сигнала передачи. Цель данной статьи — предоставить и объяснить основы цифровой обработки сигналов в радарах MIMO, представить аналитические выражения и проверить их посредством моделирования и экспериментальной верификации.*

Методы: В статье представлены теоретические основы использования дискретного преобразования Фурье (ДПФ) в качестве основного инструмента цифровой обработки сигналов для получения информации о расстоянии, скорости и азимуте цели. В пакете программ MATLAB было разработано моделирование для анализа производительности модели радиолокационной системы. Была проведена экспериментальная проверка, в ходе которой с помощью радиолокационной платформы PUP_DUAL24P_T2R4 зафиксированы конкретные сценарии, а в дальнейшем были обработаны собранные данные. Функции MATLAB, MIMOFMCW и procDC были разработаны для генерирования образцов моделирования эхо-сигналов, а также для автоматизации обработки сигналов и отображения характеристических матриц «Диапазон-Скорость» и «Диапазон-Угол».

Результаты: Моделирование и экспериментальная верификация подтверждают справедливость теоретических основ, связанных с цифровой обработкой сигналов в радарах MIMO, и позволяют четко определить целевые параметры.

Выводы: Дискретное преобразование Фурье — это простой инструмент, который дает удовлетворительные результаты для определения расстояния, скорости и целевого угла. Радарные системы FMCW обеспечивают точность в определении расстояния и скорости, в то время как режим MIMO улучшает угловое разрешение. Алгоритм DFT способен определять целевой угол, но с определенной погрешностью, что делает необходимым применение методов высокой разрешающей способности для более точного определения угла.

Ключевые слова: MIMO, радар, TDM, FMCW, куб данных радара, DFT, частота биений, виртуальная антенна.

Дигитална обрада сигнала у радарима МИМО са временски мултиплексираним сигналима на предаји

Борко Б. Ђаковић[а], *Слободан* М. Симић[б], *Лидија* М. Тривунџа[в], *Александар* Г. Ристић[г]

[а] Војска Србије, Генералштаб, Управа за телекомуникације и информатику (Ј-6), Центар за примењену математику и електронику, Београд, Република Србија, **аутор за преписку**

[б] Универзитет одбране у Београду, Војна академија, Катедра војноелектронског инжењерства, Београд, Република Србија

[в] Војска Србије, Генералштаб, Управа за развој и опремање (Ј-5), Технички опитни центар, Београд, Република Србија

[г] Министарство одбране Републике Србије, Војнотехнички институт, Београд, Република Србија

ОБЛАСТ: обрада дигиталних сигнала, телекомуникације, електроника, електромагнетика
КАТЕГОРИЈА (ТИП) ЧЛАНКА: оригинални научни рад

Сажетак:

Увод/циљ: Актуелну тему значајних истраживачких и развојних напора из области радарских система представља радарска технологија MIMO (енг. Multiple-Input-Multiple-Output). Радари MIMO представљају револуционаран искорак у домену радаске технологије, јер употребом више предајних антена које емитују ортогоналне таласне облике омогућавају бољу детекцију и угаону резолуцију. За постизање ефикасних резултата од кључног значаја је квалитетна дигитална обрада сигнала и примена напредних алгоритама како би се добиле информације о циљу. У фокусу овог рада су кохерентни радари MIMO, јер повећавају угаону резолуцију. Примењено је временско мултиплексирање сигнала на предаји, као један од основних начина постизања ортогоналности између сигнала, при чему је коришћен континуални фреквенцијски модулисани сигнал (енг. FMCW – Frequency Modulated Continuous Wave) као основа за формирање предајног таласног облика. Циљ овог рада јесте да пружи и објасни основе дигиталне обраде сигнала у радарима MIMO, изнесе аналитичке изразе и потврди их кроз симулацију и експерименталну верификацију.

Методе: Изнете су теоријске основе при чему је коришћена дискретна Фуријеова трансформација као основни алат у дигиталној обради сигнала и добијању информација о даљини, брзини и азимуту под којим се циљ налази. Развијена је симулација у софтверском пакету МАТЛАБ ради анализе перформанси модела радарског система. Спроведена је експериментална верификација, при чему су специфични сценарији снимљени помоћу радарске платформе PUP_DUAL24P_T2R4, а прикупљени подаци су накнадно *обрађени. Написане су МАТЛАБ функције MIMOFMCW и procDC за генерисање симулационих одбирака ехо сигнала и за аутоматизовану обраду сигнала и приказане карактеристичне матрице даљина-брзина и даљина-угао.*

Резултати: Симулација и експериментална верификација потврђују исправност теоријских основа које се односе на дигиталну обраду сигнала у МИМО радарима, при чему се јасно могу одредити параметри циљева.

Закључак: Дискретна Фуријеова трансформација је једноставан алат који даје задовољавајуће резултате за одређивање даљине, брзине и угла циљева. FMCW пружају тачност при одређивању даљине и брзине, а режим МИМО повећава угловну резолуцију. Алгоритам DFT успева да одреди угао циља, али са одређеном грешком, па је за тачније одређивање угла потребно користити високорезолуционе методе.

Кључне речи: MIMO, радар, TDM, FMCW, радарска коцка података, DFT, фреквенција избијања, виртуелна антена.

Paper received on: 25.11.2024.
Manuscript corrections submitted on: 26.03.2025.
Paper accepted for publishing on: 27.03.2025.